Fiber four-wave mixing source for coherent anti-Stokes Raman scattering microscopy

Simon Lefrancois,[1,*] Dan Fu,[2] Gary R. Holtom,[2] Lingjie Kong,[1] William J. Wadsworth,[3] Patrick Schneider,[4] Robert Herda,[4] Armin Zach,[4] X. Sunney Xie,[2] and Frank W. Wise[1]

[1]*Department of Applied Physics, Cornell University, Ithaca, New York 14853, USA*

[2]*Department of Chemistry and Chemical Biology, Harvard University, Cambridge, Massachusetts 02138, USA*

[3]*Centre for Photonics and Photonic Materials, University of Bath, Bath, BA2 7AY, UK*

[4]*TOPTICA Photonics AG, 19 Lochhamer Schlag, Graefelfing (Munich) 82166, Germany*

**Corresponding author: sl694@cornell.edu*

Received January 11, 2012; revised February 27, 2012; accepted March 5, 2012; posted March 6, 2012 (Doc. ID 161241); published May 9, 2012

We present a fiber-format picosecond light source for coherent anti-Stokes Raman scattering microscopy. Pulses from a Yb-doped fiber amplifier are frequency converted by four-wave mixing (FWM) in normal-dispersion photonic crystal fiber to produce a synchronized two-color picosecond pulse train. We show that seeding the FWM process overcomes the deleterious effects of group-velocity mismatch and allows efficient conversion into narrow frequency bands. The source generates more than 160 mW of nearly transform-limited pulses tunable from 775 to 815 nm. High-quality coherent Raman images of animal tissues and cells acquired with this source are presented.

OCIS codes:: 180.5655, 190.4970, 320.7140.

Coherent anti-Stokes Raman scattering (CARS) microscopy allows label-free biological imaging by exciting intrinsic molecular vibrations [1]. However, it requires two synchronized picosecond pulse trains with bandwidths smaller than the relevant Raman linewidth and a frequency spacing tunable to the Raman shift of interest. This is generally accomplished using a solid-state Nd-doped laser that is frequency doubled to synchronously pump an optical parametric oscillator (OPO) [2]. Such bulk laser cavities are complex and require careful alignment and maintenance, limiting the use of CARS microscopy outside specialized laboratories.

A turnkey source based on optical fiber technology would make CARS more accessible to its intended users. Two-color femtosecond fiber lasers can be built using the soliton self-frequency shift [3]. To maximize spectral resolution and contrast, picosecond sources are desirable. A frequency-doubled fiber source can pump a bulk OPO [4]. A two-color Er-doped fiber system was realized using highly nonlinear fiber and periodically poled lithium niobate [5]. Electronically synchronized actively mode locked fiber lasers provide rapid spectral tuning [6]. However, limited pulse energy in the former and longer pulse duration in the latter yield peak powers lower than from conventional solid-state systems.

A major challenge is to find a fiber-based frequency-conversion scheme scalable to high powers. Four-wave mixing (FWM) in photonic crystal fiber (PCF) has been used to convert 100–200 ps pulses to large frequency shifts [7,8]. However, unseeded FWM leads to large deviations from the transform limit and significant fluctuations in the converted pulses [9], both of which are detrimental to CARS imaging. Transform-limited pulses with spectra that just fill the vibrational linewidth (~10 cm^{-1}) would be optimal. For the desired few-picosecond pulses, interaction lengths are only tens of centimeters due to group-velocity mismatch (GVM), which limits FWM conversion. As a result of these issues, CARS microscopy of biological samples has not been demonstrated with a fiber-FWM source.

Here we present a fiber-based picosecond source for CARS microscopy. Frequency conversion is achieved by FWM in normal-dispersion PCF. Seeding the process mitigates the GVM and suppresses noise. Pulses from a 1 μm fiber amplifier are converted to around 800 nm with up to 160 mW of average power and durations around 2 ps. Frequency shifts in the range of 2650 to 3200 cm^{-1} have been achieved. We use this system to image mouse brain and skin tissues, as well as single cells. This is the first fiber instrument to offer performance comparable to solid-state systems.

At normal dispersion, phase-matching of the FWM process yields widely spaced and narrow bands, as required for CARS. Their position can be controlled by tailoring the dispersion of a PCF, mainly its zero-dispersion wavelength (ZDW). Figure 1 shows the phase-matching diagram for an endlessly single-mode PCF with a ZDW of 1051 nm, calculated as in [10]. The dispersion coefficients β_n at 1036 nm are 1.48 fs^2/mm, 59.5 fs^3/mm, −69.5 fs^4/mm, 136 fs^5/mm and −180 fs^6/mm. The cw pump power matches the expected pulse peak power. This shows that a pump laser tunable from 1030 to 1040 nm can be shifted by FWM in PCF to wavelengths between 770 and 820 nm with narrow bandwidths.

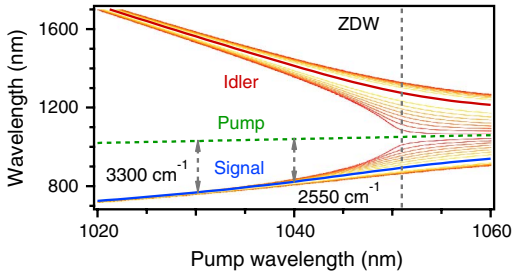

Fig. 1. (Color online) Phase-matched FWM gain for an endlessly single-mode PCF. The ZDW is 1051 nm, the nonlinear parameter $\gamma = 9.6(\mathrm{W \cdot km})^{-1}$, and the cw power is $P_0 = 3.6$ kW.

To understand the FWM process in the pulsed regime, we perform numerical simulations [11]. The simulations account for higher order dispersion, spontaneous and stimulated Raman scattering, self-steepening, and input shot noise. With only the input picosecond pump and unseeded sidebands, the process initially grows from spontaneous noise. Figure 2(a) shows the resulting spectrum after the signal field near 800 nm reaches 3.1 nJ of pulse energy, typically required for a CARS source. Broad (>10 nm), randomly fluctuating signal and idler bands develop. The signal energy saturates below 6 nJ as supercontinuum generation takes over due to non-phase-matched processes dominating beyond the GVM length. The GVM places a clear limit on the FWM process.

We propose that seeding the FWM process allows the fields to build up before the GVM separates them. Seeding is known to reduce fluctuations, but to our knowledge there is no prior report of its use to counter GVM. We simply inject cw light at the idler frequency. The resulting spectrum after 30 cm of propagation is compared with the unseeded case at similar energies in Fig. 2(a), and details are shown in Figs. 2(b) and 2(c). Significant narrowing is achieved, and the conversion efficiency is above 10%. Further conversion is limited by coherent energy exchange between fields, which generates structured pulses.

The experimental setup is shown in Fig. 3. A tunable Yb-doped fiber laser (modified TOPTICA PicoFYb) is coupled to a divided-pulse amplifier based on a 10 μm core diameter double-clad Yb-doped fiber [12]. This produces 2.5 W of pulses with 7.7 ps duration at the 54 MHz repetition rate. This is combined with a fiber-coupled diode laser tunable from 1400 nm to 1490 nm and providing up to 30 mW (TOPTICA DL pro). The polarization-matched beams are coupled into an endlessly single-mode PCF we fabricated and that matches the fiber above. Filters block the anti-Stokes light generated by mixing of the signal and pump in the PCF [13]. A fraction of the 1 μm pulses

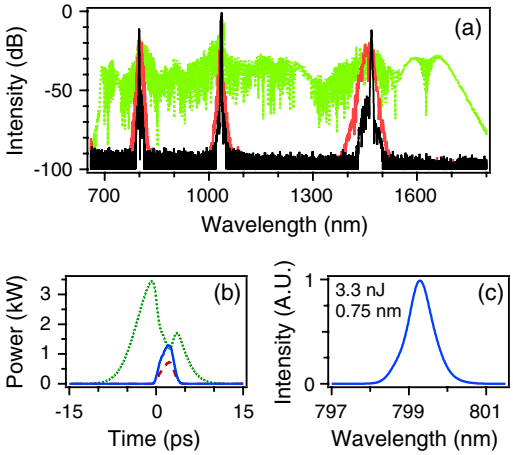

Fig. 2. (Color online) Simulated FWM. (a) Full spectrum without idler seeding after propagation through 56 cm (light solid curve) and 2 m (light dotted curve), and with idler seeded after 30 cm (black solid curve). GVM length is ~50 cm. (b) Seeded FWM: signal (solid curve), pump (dotted curve), and idler (dashed curve) pulses. (c) Signal spectrum. The input pulse is centered at 1036 nm with 7.5 ps duration and 3.6 kW peak power. Idler seed power is 5 mW at 1470 nm.

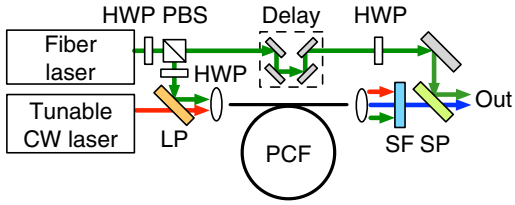

Fig. 3. (Color online) Experimental setup: HWP, half-wave plate; PBS, polarizing beam splitter; LP, long-pass dichroic mirror; SF, filters (Thorlabs DMSP1000, Chroma HQ735LP); SP, short-pass dichroic mirror.

is picked off before the PCF and combined with the polarization-matched signal at the microscope.

Experimental results with 30 cm of PCF are shown in Fig. 4. 1.6 W of pump pulses are coupled into the PCF. The idler is seeded with 5.1 mW at 1471 nm. The generated signal pulses have 166 mW of average power and a duration of 1.8 ps, while 308 mW of pump pulses are picked off. The performance is similar to solid-state systems [2]. Higher powers or longer fibers yield higher signal energies and structured spectra. The frequency difference of 2850 cm^{-1} corresponds to the CH_2 stretching vibration. With the tuning range of the diode, we achieved similar performance for frequency shifts of 2650 and 2950 cm^{-1}. By use of a similar fiber amplifier centered at 1031 nm and an amplified diode laser tuned to 1546 nm, we generated a signal wavelength of 774 nm, corresponding to a Raman shift of 3200 cm^{-1}. Coarse tuning can be accomplished by changing the pump wavelength, while fine tuning over 1 to 2 nm can be done by tuning the seed. No realignment is required.

The FWM signal and picked-off pump are coupled into a laser-scanning microscope (customized Zeiss LSM 510) and focused using a 40× water-immersion objective with NA of 1.1. We detect the forward-generated CARS signal with a nondescanned photomultiplier tube. The total power delivered to the samples is about 60 mW. CARS images at a 2850 cm^{-1} shift from a mouse ear are presented in Figs. 5(a) and 5(b). The former shows the stratum corneum at the skin surface, and the latter reveals the subcellular lipid distribution in a sebaceous gland 40 μm deep in tissue. Figure 5(c) shows a mouse brain

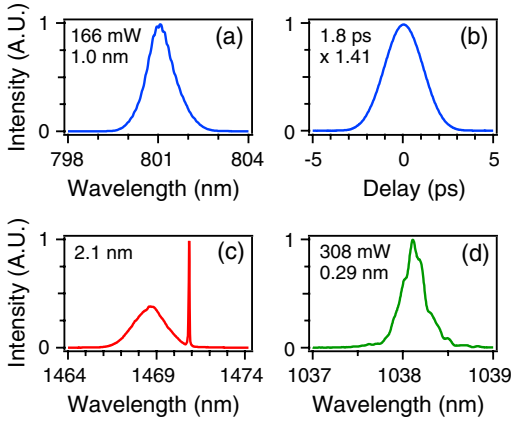

Fig. 4. (Color online) Experimental FWM results after 30 cm of PCF: signal (a) spectrum and (b) autocorrelation, (c) idler and seed. (d) Picked-off pump spectrum.

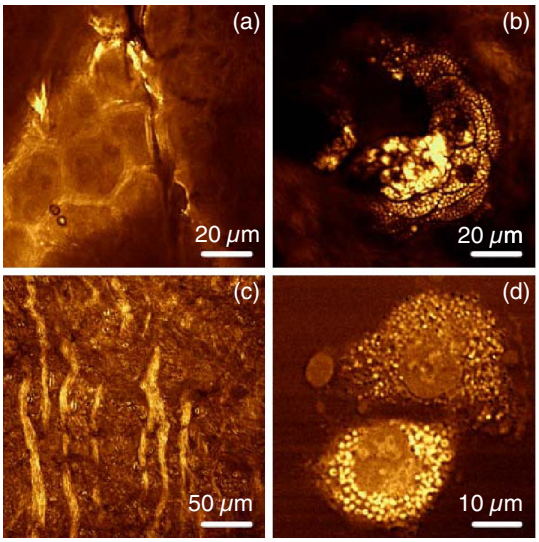

Fig. 5. (Color online) Forward-CARS images at 2850 cm^{-1}: (a) stratum corneum and (b) sebaceous gland in mouse ear, (c) mouse brain section, (d) rat fibroblasts. 512×512 pixels at 4 s/frame, no averaging.

section with the myelin sheath wrapped around the axons. Finally, Fig. 5(d) shows isolated rat fibroblast cells. The typical lipid droplet signal relative to noise is 40 for cell images and 80 to 120 for sebaceous glands, confirming image quality. At a shift of 2950 cm^{-1}, this dropped to 25 for cells and 40 for sebaceous glands.

We attempted to perform stimulated Raman scattering (SRS) imaging [14]. Preliminary experiments with dodecane showed excessive fluctuations in the SRS signal, precluding imaging. No attempt was made to design the present source for low noise, and parametric processes such as FWM amplify the noise of the pump and the seed. We can conclude that fiber sources will have to be designed for low-noise performance for SRS microscopy. Optimization of the detection scheme will also be desirable, for instance by modulating the FWM signal and detecting the quieter fiber laser pulse train.

To summarize, we have demonstrated a fiber-based source for CARS microscopy based on picosecond FWM in PCF. Seeding of the FWM process overcomes the limitations of noise and GVM. More than 160 mW of 2 ps pulses can be generated at suitable frequency shifts covering more than 500 cm^{-1}. The system could be further integrated using specialty splices and fiber couplers. This is a significant step toward a turnkey fiber-based source that will allow CARS microscopy to extend into biological and clinical applications.

This work was supported by the National Institutes of Health (EB002019) and the National Science Foundation (BIS-0967949). We thank B. G. Saar and C. W. Freudiger for help with microscopy and insightful discussions.

References

1. C. Evans and X. S. Xie, Annu. Rev. Anal. Chem. **1**, 883 (2008).
2. F. Ganikhanov, S. Carrasco, X. S. Xie, M. Katz, W. Seitz, and D. Kopf, Opt. Lett. **31**, 1292 (2006).
3. A. F. Pegoraro, A. Ridsdale, D. J. Moffatt, J. P. Pezacki, B. K. Thomas, L. Fu, L. Dong, M. E. Fermann, and A. Stolow, Opt. Express **17**, 20700 (2009).
4. K. Kieu, B. G. Saar, G. R. Holtom, X. S. Xie, and F. W. Wise, Opt. Lett. **34**, 2051 (2009).
5. G. Krauss, T. Hanke, A. Sell, D. Trütlein, A. Leitenstorfer, R. Selm, M. Winterhalder, and A. Zumbusch, Opt. Lett. **34**, 2847 (2009).
6. S. Bégin, B. Burgoyne, V. Mercier, A. Villeneuve, R. Vallée, and D. Côté, Biomed. Opt. Express **2**, 1296 (2011).
7. D. Nodop, C. Jauregui, D. Schimpf, J. Limpert, and A. Tünnermann, Opt. Lett. **34**, 3499 (2009).
8. M. Baumgartl, M. Chemnitz, C. Jauregui, T. Meyer, B. Dietzek, J. Popp, J. Limpert, and A. Tünnermann, Opt. Express **20**, 4484 (2012).
9. P. J. Mosley, S. A. Bateman, L. Lavoute, and W. J. Wadsworth, Opt. Express **19**, 25337 (2011).
10. W. H. Reeves, D. V. Skryabin, F. Biancalana, J. C. Knight, P. St. J. Russell, F. G. Omenetto, A. Efimov, and A. J. Taylor, Nature **424**, 511 (2003).
11. J. Hult, J. Lightwave Technol. **25**, 3770 (2007).
12. S. Zhou, F. W. Wise, and D. G. Ouzounov, Opt. Lett. **32**, 871 (2007).
13. M. Balu, G. Liu, Z. Chen, B. J. Tromberg, and E. O. Potma, Opt. Express **18**, 2380 (2010).
14. C. W. Freudiger, W. Min, B. G. Saar, S. Lu, G. R. Holtom, C. He, J. C. Tsai, J. X. Kang, and X. S. Xie, Science **322**, 1857 (2008).